Precision closed loop control of optical beam steering

Alfred D. Ducharme[a], Geert Wyntjes[a], Constantine Markos[a], Glenn D. Boreman[b]

[a]Visidyne, Inc., 10 Corporate Place, Burlington, MA 01803

[b]University of Central Florida, Center for Research & Education in Optics & Lasers
P.O. Box 162700, 4000 Central Florida Blvd., Orlando, FL 32816-2700

ABSTRACT

Unlike in the microwave domain, where open loop phase control is adequate, a phased array antenna (PAA) working at optical frequencies will require precise closed loop control of each element pixel to realize a well defined high brightness far-field antenna pattern. We describe and present experimental data for a design that permits precision, to $<\lambda/100$, phase control with a high bandwidth that compensates for temperature, mechanical effects, delay times of each phase shift element, and non-linear response.

Experimentally, the output of a phase measurement system is used in an electronic feedback loop to dynamically linearize an inherently non-linear liquid crystal. The experiment consisted of a spatial heterodyne, temporal homodyne, fiber optic Mach-Zehnder interferometer to recover phase of a single nematic liquid crystal element. The resulting phase measurement, represented as an analog voltage, is used in a feedback loop to correct for the non-linear drive voltage-to-phase retardance response of the liquid crystal. A demonstration of this technique using several periodic drive waveforms (sine, sawtooth, square, and ramp) at frequencies of 10-to-100 Hz was performed. Data are presented showing a phase retardance resolution of < 1 nm which enabled a significant improvement in the linearity of the liquid crystal response.

Keywords: phase measurement, liquid crystal, beam steering, optical metrology

1. BACKGROUND

The high antenna gains available at optical wavelengths make it possible to transmit signals, such as between satellites or from a satellite to a high altitude aircraft, at rates as high as 1 Gbit/sec. Distances in excess of 500 km can be achieved with lightweight transmitters and receivers having apertures only a few inches in diameter. These laser communications or lasercom links are also highly secure, virtually jam proof and have, because of their high frequency, a high degree of immunity from severely disturbed atmospheres, e.g., due to a nuclear event. However, exquisite pointing precision and stability are required to acquire the transmitted signal and maintain the link in the presence of mechanical vibration, thermal influences, and disturbances such as atmospheric turbulence. Since many of these disturbances have substantial frequency content, up to 1 kHz, this calls for a pointing capability that is highly agile. An optical phased array antenna is ideally suited for this, either as a freestanding system or as an adjunct to a steering mirror to provide high frequency, small angle pointing corrections.

Limitations of mechanical beam steering and stabilization mechanisms and the potential advantages of optical phased arrays are discussed in a survey paper by McManamon et al.[1] They note that, despite considerable effort over many years, mechanical beam steering remains complex, requires precision mechanisms, and is expensive. The mechanisms frequently are massive, and therefore are not suitable for rapid and/or random-access pointing. Prohibitive amounts of drive power are often required for slewing and troublesome amounts of torque may be produced on flight vehicles. In contrast, optical phased arrays typically require little power for rapid beam slewing. They are inherently random-access devices, and do not contain large moving masses. Their costs can potentially drop rapidly with volume production.

Phased array radars are common at microwave frequencies, e.g., L-band and X-band. They are used for long

range target acquisition and tracking, as well as on tactical aircraft as part of the fire control system. Their advantages are much greater agility and faster scanning than a mechanically steered system, and the ability to track multiple targets simultaneously. An optical phased array system would have the same advantage of a diffraction limited field of view that could be steered over large angles virtually inertia free. Conceptually, optical and microwave arrays are identical except that an optical system operates at much higher frequencies (f=300 THz, λ = 1 micron) vs. an L-band radar (f=1.5 GHz, λ=20cm), or a factor of 2×10^5 shorter wavelength. The optical phased array has the advantage that the phase of each array element, $\Delta\phi=\Delta x/\lambda$ cycles, can be changed significantly with very small changes in physical distances Δx. It follows that for a high quality exit beam, with low ripple and side lobes, the errors in x should also be small, e.g., $< 10^{-2}\lambda$. For example, at λ=1 micron, $\Delta x \leq 10^{-2}$ micron (10 nm). For large numbers of elements and high scan rates, this represents a difficult task and requires closed loop control, using some kind of measurement or metrology system to determine these distances or phases. For a microwave system, because of the much longer wavelength, open loop control is, in general, adequate. This aspect of optical phased array antennas is discussed in papers by McManamon et al.[1,2]

There is another area of fundamental difference. The phase of an optical signal cannot be measured as an electric field E(x,t) using an antenna, but, because of the much shorter wavelength, must be recovered as an intensity I(x,t) through interference with a reference beam. Each exit phase must therefore be compared against a common reference beam, so the relative phases can be adjusted and controlled.

1.1 Beam steering

The general concept of an optical phased array is illustrated in Fig. 1. An input plane wave is incident on an array of phase shifting elements. The elements of the array are set to produce a transmission blaze grating. In this illustration 16-elements are utilized to produce a two period blaze grating. The effect is an output wave that is effectively steered or redirected in the far-field.

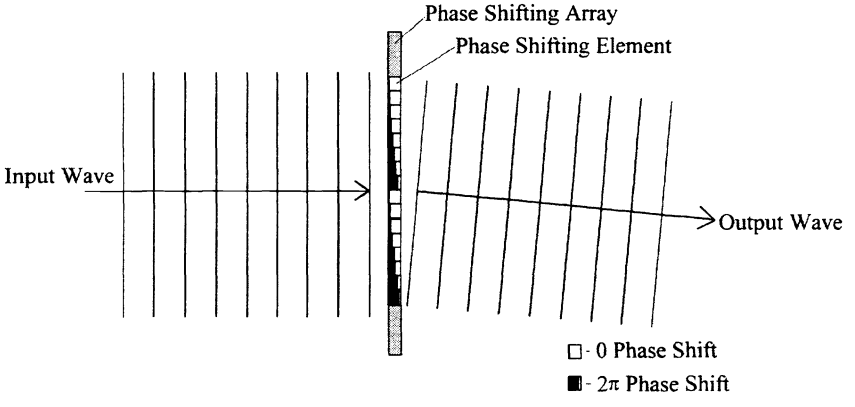

Figure 1. Beam steering using optical phased array.

Given a sufficient number of properly spaced sub-apertures, the contributions from each element or sub-aperture will superimpose to form a planar output wavefront with a deflection angle θ given by:

$$\sin\theta = \frac{\lambda\Delta\phi}{D} \qquad (1)$$

where $\Delta\phi$ is the phase offset in cycles of adjacent sub-apertures and D is the center-to-center spacing of the sub-apertures. The deflection angle, which changes with the phase offset, can be varied at a rate limited only by the time response of the phase-shifters.

1.2 Open loop vs. closed loop beam steering

The problem that arises when using an optical phased array is that small phase delay errors between the commanded phase shift and the actual phase shift of each phase shifter in the array can greatly reduce the encircled power at the target plane. This problem is illustrated in Fig. 2.

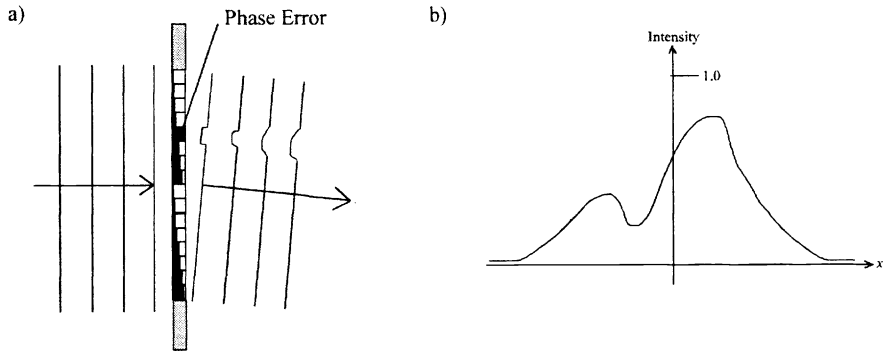

Figure 2. Optical phased array with small phase error in a single pixel a) and the resulting far-field intensity pattern.

A small phase error is introduced to a single phase shifting pixel (exaggerated in the figure). This causes a delay in the wavefront which results in the formation of a side-lobe in the far-field pattern. The phase error can be caused by small temperature variations which shift the voltage response of each pixel. Using a feedback loop, which measures the phase error of each individual pixel, the wavefront can be corrected.

In this project Visidyne has demonstrated the potential for three innovations that are expected to greatly improve on the practical aspects of implementing a true optical phased array system. These are:

1. Separating and decoupling the functions of the power, or transmitter laser (or local oscillator laser in case of a receiver) from the task of controlling exit phases of the array, that is, the metrology function.
2. A novel approach for measuring the relative phase angle between reference and exit beams utilizing baseband, homodyne (as opposed to heterodyne) measurements to provide a fast > 1 MHZ measurement at high resolution (<<1° or <1 nm).
3. Using the chirping or large wavelength tuning capabilities of laser diodes, as a means of adjusting absolute path length and therefore phase for each element. This is important in case the primary laser is tuned over a wide spectral range. Unless the absolute path length to each exit aperture of the array is well equalized, "squinting" will occur, in which the beam collimation degrades as the wavelength is varied.

2. EXPERIMENTAL SET-UP

The goal of the experiment performed in this project was to demonstrate the ability of the Visidyne Digital Phase Processor to be used in a high-speed feedback loop. To achieve this, the Center for Research and Education in Optics and Lasers (CREOL) and Visidyne assembled an optical breadboard Mach-Zehnder interferometer to study the behavior of a single pixel nematic liquid crystal phase modulator. As shown in Fig. 3, the system utilized a FiberBench source manufactured by OFR. The FiberBench collimates the output of a Sharp LT015, 40 mW, 820 nm laser diode across a 5 cm free-space bread-board area into a fiber coupling lens. A Faraday optical isolator, polarizer, and tweaker plate were used on the OFR bread-board area to condition the light emitted by the laser diode and to isolate the laser from back reflections. The coupling lens focuses the light onto a single-mode (5 um core) polarization maintaining optical fiber.

A waveguide phase modulator (WPM) was used to divide the output optical fiber equally into two single-mode optical fibers. The output of the feedback circuit was low-pass filtered and used to drive the WPM. This stabilized the effect of slow temperature fluctuations which causes the fringe pattern to drift. Two New Focus Fiber Aligners were used to launch the output of the optical fibers. The first beam was transmitted through the combining beam splitter onto an fringe detector and represents the 'reference' path of the interferometer. The second beam is transmitted through a single element liquid crystal. The, 'signal' beam is then reflected by the combining beam splitter onto the fringe detector. The signal and reference beams interfere to produce a spatial fringe pattern with a fringe spacing expressed as,

$$L = \frac{\lambda}{\theta} \tag{2}$$

where θ is the angle (in radians) between the two beams and λ is the wavelength of the source.

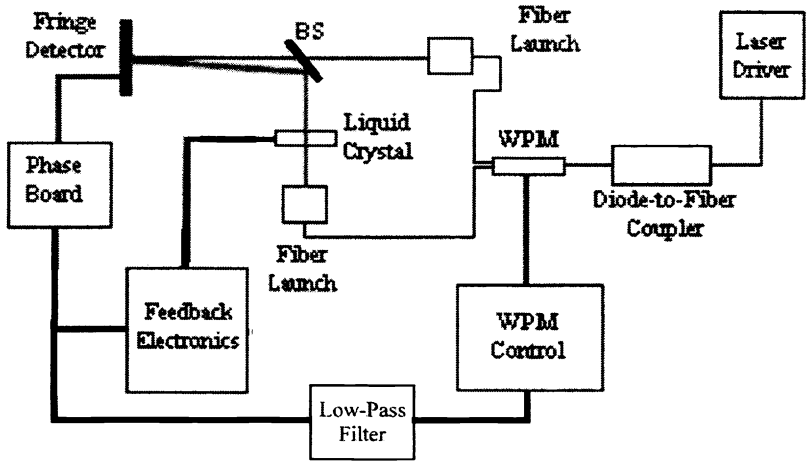

Figure 3. Diagram of optical bread-board experimental set-up.

2.1 Fringe detector

The fringe detector is a linear photodiode array containing 30 elements which sample the fringe pattern. The angle between the reference and signal beams was adjusted to achieve a fringe spacing equal to the width of three detectors. This provides three samples of a single period of the fringe pattern with a center-to-center spacing of 120°.

2.2 Phase processor

The output signal from the fringe detector is converted to a digital phase value corresponding to fringe shift using the Visidyne Digital Phase Processor (DPP). The DPP, which is a Visidyne proprietary device, was originally designed for precision phase measurements of signals from optical interferometers. The phase processor performs three basic functions: (1) The fringe detector input voltages are converted to a digital word proportional to phase. (2) The phase is "unwrapped"; that is, cycles are counted so that the phase word is continuous over many cycles of phase change. (3) The phase data are digitally low-pass filtered to improve the signal-to-noise ratio of the phase data.

2.3 Liquid crystal phase modulator

The intent of this project was not to improve upon the performance of a liquid crystal phase modulator but rather to correct the linearity of a commercially available modulator. The liquid crystal purchased and used for this experiment was manufactured by Cambridge Research & Instrumentation, Inc. (CRI) and distributed by Thor-Labs Inc. The Model CR-300 single element Phase Modulator has the following specifications:

Modulation	500nm phase modulation
Speed	100 ms for full modulation
	10 ms for 50 nm step
Maximum input power	25 mW
Spectral range	430-780 nm
Transmission	> 85%
Reflection	< 2%
Temperature	+15 to +40 C ambient
Input aperture	5 mm diameter

The specified spectral range of the CR-300 was just below our wavelength of 820 nm. After talking with engineers at CRI, they assured us that the device would still operate at our wavelength and this was verified during our experiment. The device is housed in a 2.75" x 2.75" X 1.80" enclosure which contains all necessary drive electronics. There is a single modulation input, BNC, connection that was used to input an analog drive voltage.

2.4 Feedback electronics

The fringe detector generates the voltage signal which was used by the phase board to determine fringe shift. The output rate of the phase board is 4 MHZ and performs the equivalent of an average of 256 samples using the digital filter. This equates to a 15 KHz throughput rate. The 16-bit digital output of the phase board was converted to an analog waveform using an AD669 digital-to-analog converter. The 4 MHZ clock on the phase board was divided down using a ripple counter to 15 KHz which was used to clock the AD669. Since the relative speed of the liquid crystal was approximately 100 Hz, the rate of the feedback system was several times faster.

The feedback electronics consisted of a subtractor circuit where the negative input to the operational amplifier came from an HP function generator and the positive input came from the phase board. The output was connected directly to the liquid crystal which was the difference of the two inputs. The output of the subtractor circuit is given by,

$$v_o = v_{\Phi_{Bd}} - v_{Fn\ Gen.} \tag{3}$$

The gain of the subtractor was adjusted to increase the effective loop-gain of the feedback loop to approximately 100.

3. EXPERIMENTAL RESULTS

A series of measurements were used to study the performance of the overall system. First, the system was tested in 'open-loop' mode to determine the phase resolution and transfer function of the system. Second, several 'closed-loop' measurements were performed to determine the ability of our feedback loop to 'linearize' the liquid crystal.

3.1 Open loop measurements

3.1.1 System noise characterization

The data obtained to characterize the noise is shown in Figure 4a and b. A file of 1000 phase words was acquired from the digital output of the phase processor board and the data are displayed in histogram form in Figure 4a.

The digital filter time constant was set to 1 ms and the data were sampled at 6.1 kHz by a PC. The histogram shows a shoulder due to slow drifts of the laser wavelength (a TE cooler was not used and therefore the 2 beam interferometer was not optimized). The main peak in the histogram has a FWHM of approximately 0.0002 cycles which is consistent with a phase resolution of 1.0 x 10^{-6} /$Hz^{1/2}$.

The corresponding power spectral density (PSD) of the data was calculated and is shown below in Figure 4b. The power density falls off at higher frequencies eventually leveling out at about 1 kHz (for a digital average of 4096) at a value of 1.0 x 10^{-12} Hz^2/Hz in power and a corresponding phase amplitude resolution of 1.0 x 10^{-6} Hz thus indicating a noise floor.

a)

b)

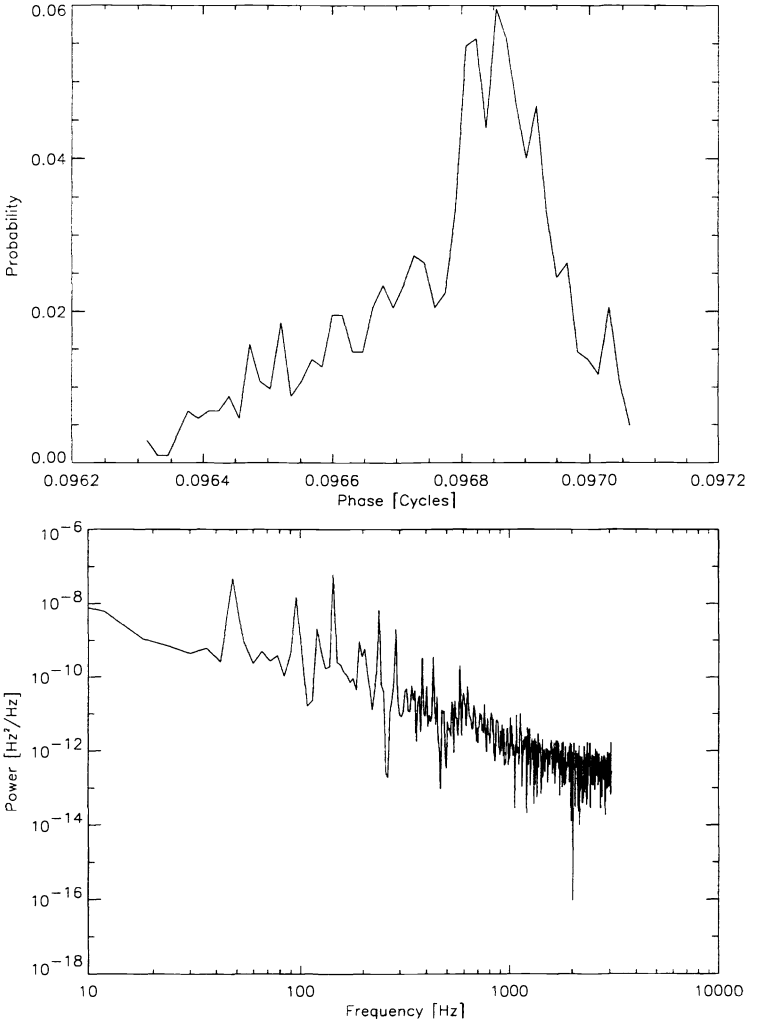

Figure 4. Histogram of system phase variations a) and corresponding Power Spectral Density (PSD) corresponding to the above histogram data b).

3.1.2 Bandwidth

The bandwidth of the system was measured and found to be limited not by the speed of the ADC as expected but instead by the choice of the focal plane array amplifiers and the size of the photodiode detector elements. A 1-volt sinewave modulation was injected into the waveguide modulator and the corresponding phase modulation was measured by observing the analog output from the phase processor board. The frequency of the input modulation was varied

between 1 kHz and 250 kHz. The system response was measured at 16 different frequencies which are plotted in Figure 5. The response is seen to be essentially flat out to 100 kHz before rolling off to approximately 6 db at 200 kHz.

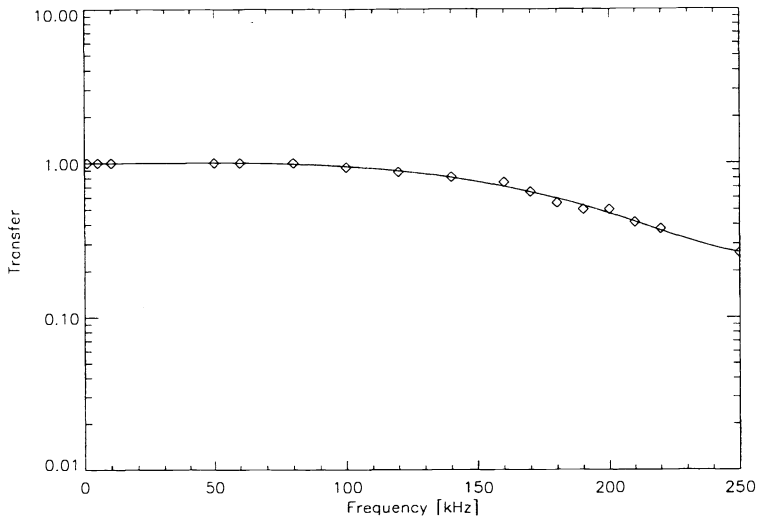

Figure 5. System Response as a function of frequency.

3.1.3 Liquid crystal response

The phase retardance-to-voltage response curve for the liquid crystal is inherently non-linear (see Fig. 6).

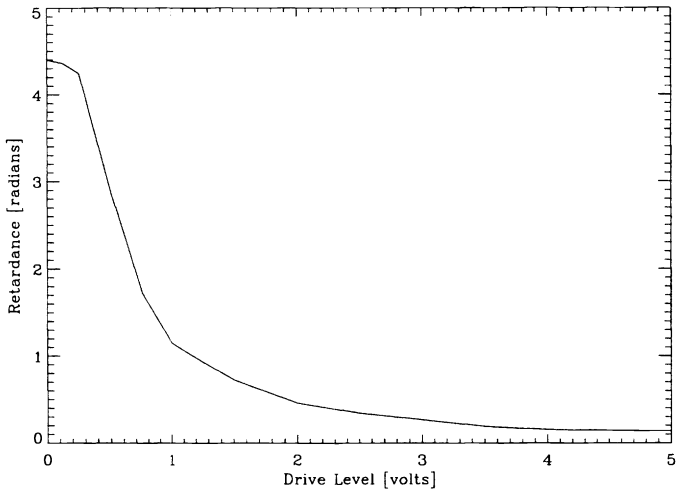

Figure 6. Liquid Crystal voltage response at operating wavelength of 820 nm.

The objective of the closed loop measurements was to linearize the effective response of the liquid crystal.

The time response of the liquid crystal was measured to test the ability of the CR-300 phase modulator. In addition, this measurement demonstrates a potential commercial application of our technology as a diagnostic tool for quality control of phase modulation devices. The data shown in Fig. 7 was taken using the CR-300 and the phase measurement system. A 50 Hz, 5V , square wave was used as a drive input to the liquid crystal. This waveform along with the corresponding phase measurement are plotted.

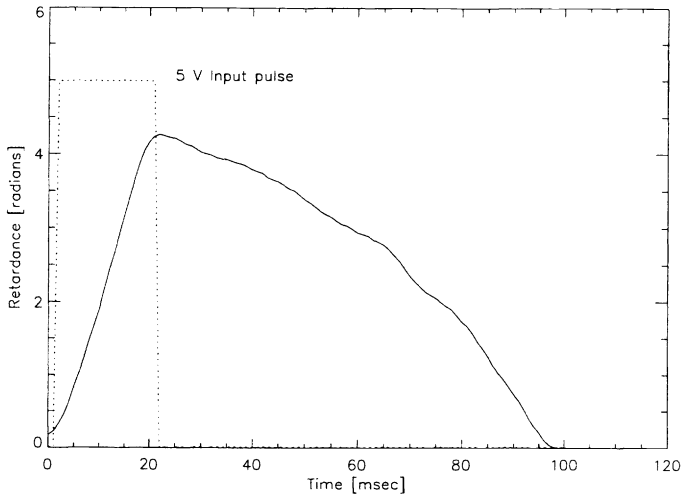

Figure 7. Time response measurement of CR-300 liquid crystal phase modulator.

This measurement shows that the CR-300 has approximately a 20 msec rise-time and an 80 msec fall- or relaxation -time.

3.2 Closed loop measurements

The system closed loop response was measured to demonstrate the ability of our technology to measure the phase induced by a phase shifting device with a high bandwidth at KHz rates. A switch on the feedback electronics allowed the system to be opened and closed so that the improvement in the linearity of the liquid crystal response could be observed and recorded. Several different drive waveforms were used as inputs to the CR-300 phase modulator. An HP waveform generator was set for a 0-to-1 V output. The same 300 Hz frequency was used for all waveforms. Figure 8a-d shows both the open and closed response of the system.

A significant improvement in the linearity of the liquid crystal can be seen in Fig. 8. Figure 8a shows a square wave which has a reduced width. Figure 8b and d show a triangle and sine wave respectively. An important difference between these curves is their peaks. The triangle is more pointed and the sine wave more rounded. Unfortunately, the time response of the liquid crystal limits the ability of our system to correct for it's non-linearity.

4. CONCLUSIONS

This effort demonstrated the basic premise that, while conceptually an Optical Phased Antenna Array (O-PAA) is similar to a microwave design, the greatly reduced wavelength at optical frequencies requires a radically different approach in the detection and control of the phase between elements of the array. While at microwave frequencies and in the mm waveband open loop control is adequate, closed loop control using a built in metrology capability is a requirement to realize the requisite precision for the far field antenna patterns.

We have demonstrated that precise phase, path length control to $\lambda/256 \approx 3$ nm could be dynamically controlled in the presence of vibrations and compensate for the non-linear response of the phase shifters in the form of a Liquid Crystal (LC) element. Future work will extend the technique to a large number of pixel elements, mandatory for an eventual system application.

The technology we have demonstrated can also benefit the phase modulator manufacturing industry. The system could be easily modified into an optical metrology tool used to test the performance of all types of optical phase modulators. This system could provide dynamic real-time feedback which would decrease development time and increase manufacturing yield.

a)

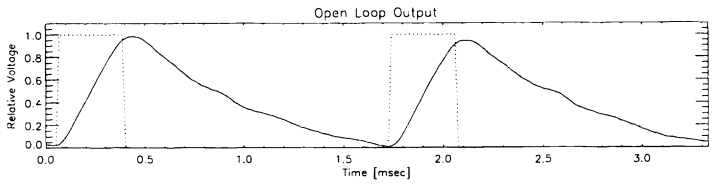

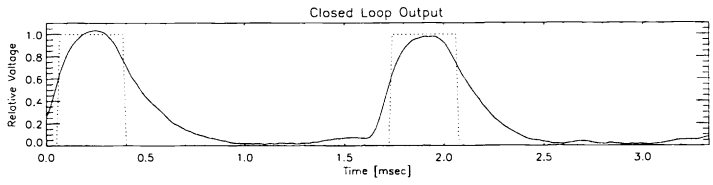

b)

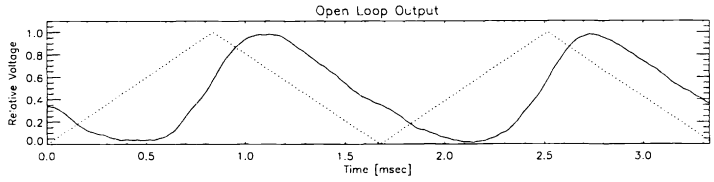

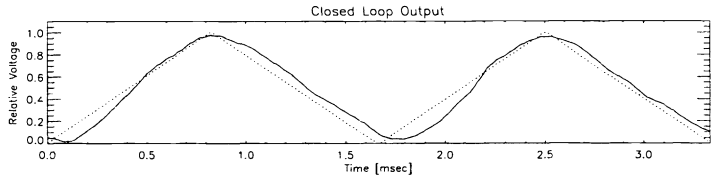

c)

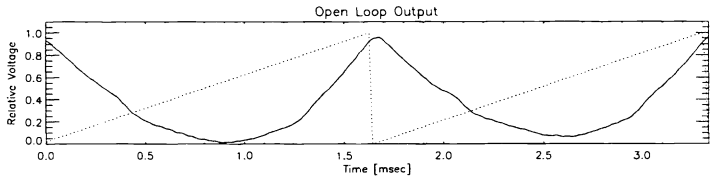

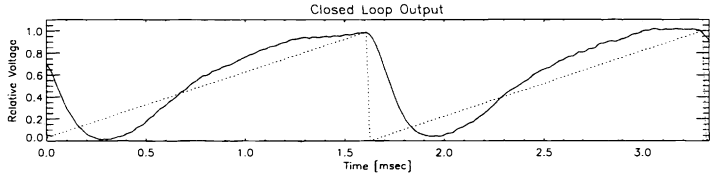

d)

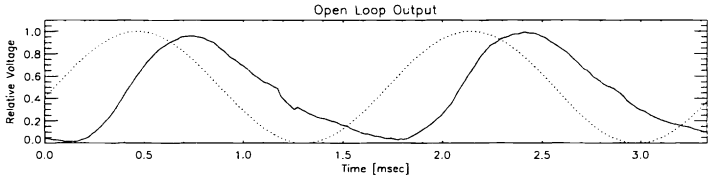

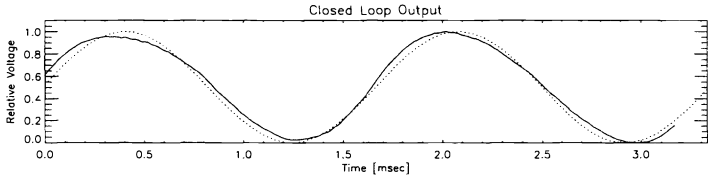

Figure 8. Experimental results for 300 Hz input wave (dotted line) and output wave (solid line) for a) a square wave, b) triangle wave, c) ramp wave, and d) sine wave.

5. ACKNOWLEDGEMENTS

This work was supported by the Small Business Innovative Research program (SBIR) under the direction of the U.S. Air Force Wright Laboratory Contract F33615-96-C-1952.

6. REFERENCES

1) P. McManamon, T. Dorchner, D. Corkum, L. Friedman, D. Hobbs, M. Holz, S. Liberman, H. Nguyen, D. Resler, R. Sharp, and E. Watson, "Optical phased array technology", *Proceedings of IEEE*, v. 84, No. 2, pp. 268-298, 1996.

2) W. Neubert, K. Kudielka, W. Leeb, and A. Scholtz, "Experimental demonstration of an optical phased array antenna for laser space communications," *Appl. Opt.*, 33(18), pp. 3820-3830, 1994.